Geodesy and Geodynamics 9 (2018) 187–196

Contents lists available at ScienceDirect

Geodesy and Geodynamics

journal homepage: http://www.keaipublishing.com/en/journals/geodesy-and-geodynamics/

The deforming and rotating Earth – A review of the 18th International Symposium on Geodynamics and Earth Tide, Trieste 2016

Carla Braitenberg

University of Trieste, Department of Mathematics and Geosciences, Via Weiss 1, 34100, Trieste, Italy

ARTICLE INFO

Article history:
Received 1 January 2018
Received in revised form
20 February 2018
Accepted 15 March 2018
Available online 29 March 2018

Keywords:
Geodynamics
Earth tides
Geodetic observation
Earth rotation parameters
GNSS

ABSTRACT

The 18th International Symposium on Geodynamics and Earth Tides 2016 covered phenomena that generate temporal variations in geodetic and geophysical observations. In calculating the stress field for Earth tides, the observed geodetic response is used for defining the Earth's rheology, the Earth internal structure, Earth rotation parameters, and the functioning of the sophisticated instrumentation mounted on Earth and satellites. The instrumentation capable of observing Earth tides, measures changes generated by lithospheric plate movements, as the earthquake cycle and volcanism. Hydrology, temperature, and pressure, either of natural or anthropogenic origin, affect the high precision observations, and therefore must be included in this study-realm.

1. Introduction

In the week of 5–9 June 2016, the 18th International Geodynamics and Earth Tides Symposium "Intelligent Earth system sensing, scientific enquiry and discovery" was held at the University of Trieste, in Trieste, Italy, with over 106 presentations. Here a review of the topics discussed at the Symposium is given, with the aim of documenting the rich spectrum of international research activities on these interdisciplinary subjects.

The meeting was the first in which the word *GEODYNAMICS* was added to the classical Earth Tide Symposia, held since 1957. The Symposia were connected to the ICET (International Centre of Earth Tides), which was first housed at the Royal Observatory of Belgium at Brussels, and then was moved to the University of French Polynesia, Tahiti [1] (page 767). The topics of the Earth Tides Symposia have been increasingly linked to geodynamics, leading to the transformation of the IAG (International Association of Geodesy) Scientific Service ICET [2] to the IGETS (International Geodynamics and Earth Tides Service) [3], with its Central Bureau hosted at EOST in Strasburg (Ecole et Observatoire des Sciences de la Terre, University Strasbourg, France) and the database held at GFZ (Deutsches GeoForschungsZentrum) Potsdam [4]. The transformation reflects the instrumental innovations and broadened applications of terrestrial and spaceborne geodetic monitoring, instruments that are sensitive to Earth tides. Together with ICET, the GGP (Global Geodynamics Project) which is responsible for supporting research activities using the data from the worldwide network of superconducting gravimeters, was also merged into IGETS.

The 2016 Symposium addressed a wide range of scientific problems in geodynamics research and chose the theme of "Interactions of geophysical fluids with Earth tides phenomena and observations" as a specific focus. The themes were enveloped in the seven sessions of the Symposium. Here a review on the topics discussed at the Symposium is given, which demonstrates the broad spectrum of applications of terrestrial and space geodetic observations of Earth geometry, crustal deformation, Earth global shape parameters, Earth rotation parameters, the gravity field and the temporal changes of these effects.

2. Review of the topics presented at the symposium

2.1. Tides and non-tidal loading

The opening session on tides and tidal loading discussed the tidal signals observed in a number of stations with laser

E-mail address: berg@units.it.

Peer review under responsibility of Institute of Seismology, China Earthquake Administration.

Production and Hosting by Elsevier on behalf of KeAi

https://doi.org/10.1016/j.geog.2018.03.003

extensometers, water tube tiltmeters, ocean bottom and land spring gravimeters and SG (superconducting gravimeters). The fact that the tidal deformation and gravity signal can be calculated and has well defined spectral frequencies, makes the tidal signal a powerful tool to test instrument performance, recover local rheological crustal properties, and test the ocean tidal models through the observed loading tides. Table 1 lists the tilt and extensometric stations mentioned in the text. The location of the stations from Table 1 are displayed in Fig. 1, which shows also the network of the SGs (personal communication S. Rosat).

The Earth elastic response to tides, loads and stresses is expressed by the corresponding Love-Shida numbers. Varga et al. [30] presented the theory to calculate relations between these numbers with an integral approach. The authors analyzed the tidal stresses from Earth surface to the core-mantle boundary with the aim to determine the triggering effect of tides on earthquakes [31].

The SGs have lower noise levels than the quietest seismometer station for frequencies below 1 mHz and above 6 mHz, as was shown by comparing the noise spectra to the "low noise seismologic model" [32]. The SG is, therefore, an ideal instrument in searching for low frequency gravity signals as the Slichter modes [33]. The SGs being relative instruments, their amplitude factor, phase delay and long-term drift must be determined. It was found that the theoretical and observed amplitude ratios at tidal spectral frequencies are stable and independent of local effects, and are precise enough to verify the stability of the SG scale factor. The instrumental drift of the SGs is determined by absolute gravimeters in order to extract long term gravity changes [34–36]. Crossley and Murphy [37] and Wziontek et al. [38] found evidence of the hydrological signal in SG decades-long time series in the order of $\pm 100 \times 10^{-9}$ m/s^2 in case of the Apache Point observatory (elevation 2788 m, Sunspot, New Mexico, USA), with trends of 4×10^{-8} m/s^2/year [37] after having corrected for a global hydrologic mass model. The Apache Point Observatory station serves a lunar laser ranging telescope site and it is necessary to determine the regional rheological properties of the crust, in order to determine predicted surface movements at high precision using SG and GPS. At station Medicina (Italy), an extensive tidal analysis was performed after removing long term gravity effects due to crustal deformation obtained from GNSS time series. Independent parameter sets for the degree 3 tidal potential and the 18.6 years tidal constituent of the Moon were considered (Wziontek et al. [38]). The tiltmeter stations of St. Croix and Rustrel, France record similar signals correlated to water springs, and the karstic environment in which they are set, and have hydrologic signals with amplitudes of several hundred 10^{-9} rad in St. Croix and in Rustrel [7,39].

The Argentinian-German Geodetic Observatory, housing an absolute gravimeter and an SG next to GNSS, VLBI and SLR stations, senses the influence of the Rio de la Plata (river and estuary formed by the confluence of the Uruguay and the Paraná rivers, at the border between Argentina and Uruguay). The effect of storm surges on the SG was successfully modeled [40]. The non-tidal component constitutes 88% of the signal, 12% being the tidal amplitude contribution. After correcting for the storm surge, a hydrologic signal correlated to rainfall emerged.

The ocean loading tides were calculated with different approaches, as the ocean tide loading calculation service of Georg Scherneck (http://holt.oso.chalmers.se/loading) used e.g. in the Lohja station, Finland, or the convolution of the ocean tide models with the ocean loading Green functions [41] used e.g. in the Canfranc, Spain station. Amoruso and Crescentini [5] could identify the presence of nonlinear and minor ocean tides from the localized mismatch of the observed and modeled tidal signals in the underground laser extensometers of Canfranc, more than 120 km from the Bay of Biscay. The signals were quantitatively compared with computations using TPXO8 (MN4, M4, and MS4) and FES2012 (M3, N4, MN4, M4, MS4, and M6) global ocean tide models.

The ocean loading tides were also theoretically considered on GPS stations to find anelastic effects in terms of the Q-value of the crust, which was interpreted as due to interstitial fluid flow in

Table 1
Extensometer and tiltmeter stations discussed at the Symposium.

Station name	Instrumentation	Year of installation	Abstracts and reference
Canfranc, Spain	Laser extensometers, 70 m length	2011	[5,6]
St. Croix, Vosges mountains, France	Long base water tube tiltmeter, 100 m length	2004	[7,8]
BFO, Schiltach, Germany	Horsfall watertube tiltmeter, 110m length; Invar wire strainmeters 10 m length		[7,9–11]
LSBB, Rustrel, France	Long base water tube tiltmeter	2012	[7]
Tytyri mine,Lohja, Finland	Long base interferometric water level tiltmeter (code NSiWT), 50.4 m length	2008	[12,13]
Metsähovi, Finland	Research borehole for vertical tilt meters, 2 Superconducting gravimeters collocated with FG5X absolute gravimeter and hydrological monitoring	1985	[14,15]
Conrad observatory, Austria	Interferometric water level tilt meter, 5.5 m length (code W_iWT); Lippmann 2D tiltmeter	2014	[16]
California and Nevada	11 long base interferometric extensometers, 380 m to 730 m length	Starting 1976	[17]
Ksiaz-Warsaw, Poland	Water tube tiltmeter, quartz tiltmeter, extensometer, 60 m to 94 m length		[18]
Grotta Gigante, Italy	Horizontal pendulums, 95 m top and bottom height difference, colocated Marussi tiltmeter, 0.7 m horizontal baseline.	Starting 1960	[19]
Grotta Genziana, Italy	Marussi tiltmeter, 0.7 m horizontal baseline.	Starting 2007	[20]
Baksan Observatory, Elbrus volcano, northern Caucasus	Baksan Laser interferometric strainmeter, 75 m length		[21]
Geodynamic Observatory Moxa, Germany	Quartz-tube and laser strainmeter (3 directions), up to 38 m length, Askania borehole tiltmeters, up to 100m deep. Research borehole (20 m and 100 m deep) for injection pumping, superconducting gravimeter.	1964 1997 2012 1999	[22,23]
Sopronbánfalva Geodynamic Observatory, Sopron, Hungary	Quartz-tube extensometer, 22 m length	1990	[24,25]
Mátyáshegy Gravity and Geodynamic Observatory (Budapest, Hungary)	Two quartz-tube extensometers E1 (21.3 m length) and E2 (13.8 m length)	1980	[26]
Pécs station in uranium mine (Pécs, Hungary)	Quartz-tube extensometer, 20.5 m length	1990–1999	[24,27]
Vyhne Tidal Station (Vyhne, Slovakia)	Quartz-tube extensometer, 20.5 m length	1980	[28,29]

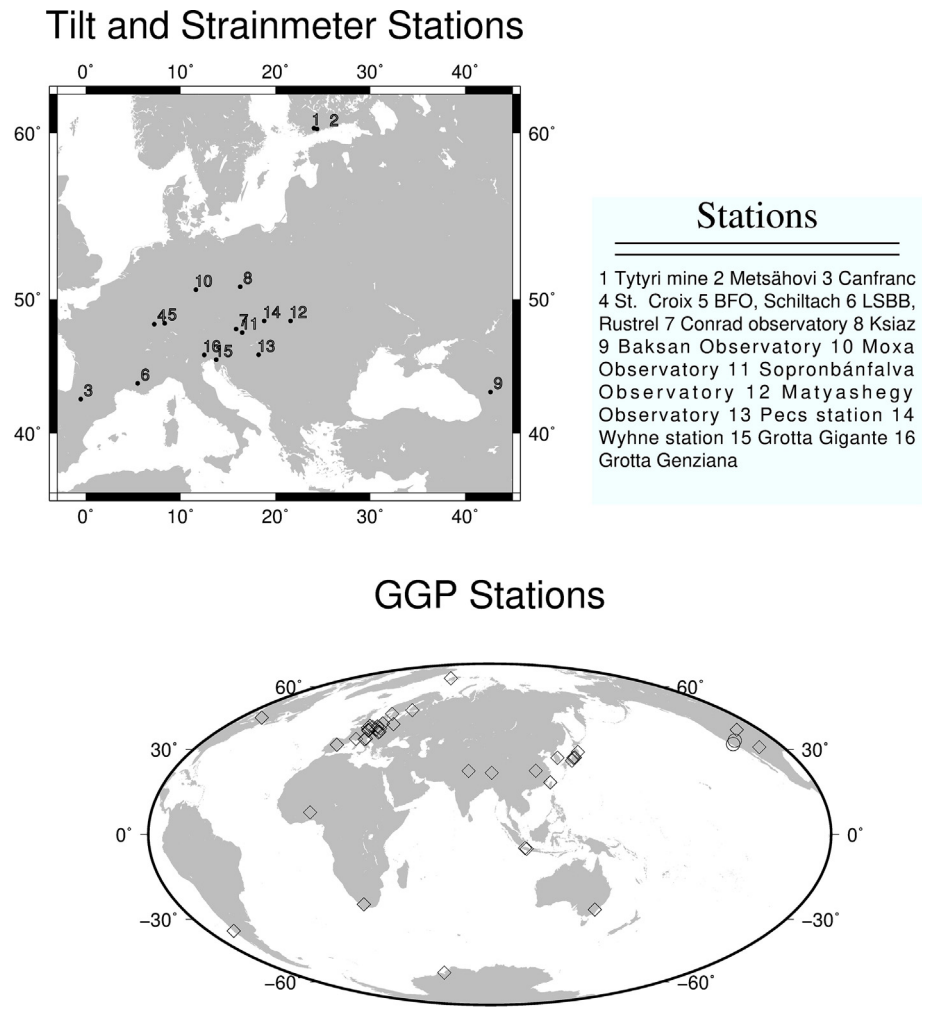

Fig. 1. Location of Tilt and Strain meter stations (Circles) mentioned in the text and location of the Superconducting gravimeters (diamonds) of the Global Geodynamics Project. The two circles in the GGP-world map are the two extensometer stations of California and Nevada mentioned in the text, respectively.

cracks [42]. Boy et al. [43] successfully implemented atmospheric, non-tidal oceanic and hydrological loading in the GAMIT station-processing software. They found that for globally distributed GPS stations a large part of the variability cannot be explained by the loading effects, and that the continental global hydrology model GLDAS [44] has missing components.

Earth tide spring gravimeters are easily installed and do not require particular laboratory equipment as does the super-conducting gravimeter. Zahran et al. [45] reported an experiment of two continuously measuring Earth tide gravimeters installed close to the Nasser Lake, with the aim to distinguish subsurface water movements and possible relations to the seismicity. It seems that seismicity is increased following the periodic water level change of the lake. First results showed that the gravity signal must be corrected for the vertical movements and the lake mass changes, before conclusions on the subsurface mass changes can be made.

Between 2009 and 2016 many efforts were made to upgrade the obsolete gravimetric instrumentation (based on Lacoste Romberg (LCR) G type gravity meters) of Hungary with the aim to determine the location-dependence of the bulk tidal effect in the Pannonian basin at diurnal and semi-diurnal bands. 5 spring type (4 LCR G and 1 Scintrex CG-5) and 1 cryogenic (SG025 of Conrad Observatorium, Austria) gravimeters were used at 5 locations to record 3–12 month long time series in a mainly co-located setup. Although many of the possible instrumental problems [46,47] and environmental (especially the microseismic noise) effects were considered carefully [48] and even the moving mass calibration method [49] was applied to provide accurate scale factors, direct comparison of tidal amplitude factors was not considered to be feasible. Therefore rather the tidal amplitude ratios O1/M2 were examined. The results consisted in a weak (0.2%) increase of the ratio from west to east, in agreement with the theoretical considerations [47].

A sea floor gravimetric recording above the Troll A gas reservoir in the North Sea off-shore Norway was analyzed together with an ocean bottom pressure sensor. The signals were predicted with solid tides, the FES2014v ocean model, and a dynamic model of sea level response to atmospheric pressure and wind forcing [50].

Repeated gravity measurements over a geodetic network centered on the Vrancea seismic area in Romania found a relative gravity decrease of −0.06 mGal in 20 years (−3 microGal/yr) centered on the seismic area with respect to the stable surrounding reference points. The result is interpreted as due to mass decrease at lower crustal levels connected to the subduction of the Vrancea [51]. The size of the gravity change is comparable in amplitude to that found in Tibet, at Lhasa station, where repeated absolute gravity measurements have been made for several years, and gravity is also measured continuously using an SG. The time series of the SG at Lhasa has been controlled with an absolute gravimeter, and shows that Lhasa gravity is decreasing by a rate of 1.87 microGal/yr, with a GPS recorded uplift of 0.8 mm/yr, resulting in a gravity uplift ratio of −23.375 microGal/cm [52].

Earth tidal measurements by quartz tube extensometers of the same type were performed at several observatories (Budapest, Pécs, Sopronbánfalva in Hungary and Vyhne in Slovakia). The effect of the Free Core Nutation (FCN) on the P1, K1, Ψ1 and Φ1 tidal waves were studied on the basis of tidal results obtained in the four observatories. The effectiveness of the correction of tidal data for temperature, barometric pressure and ocean tide load was also investigated [24]. One effect of the FCN is to reduce the ratio of the P1 to K1 to 0.96 of the tidal potential. Agnew [53] reported this effect can be detected in the harmonic constants for ocean tides and could have been detected already in from observations related to the interval 1930 to 1980.

Tidal analysis of the extensometric data in the Vyhne Tidal Station between 2005 and 2015 revealed that the measured tidal amplitudes are close to the theoretical values. The effect of the local conditions, such as structure of the observatory, cavity effect, topography and geologic features of the surrounding rocks, was investigated in detail and these effects were taken into consideration during the interpretation of the results of the data analysis [29].

The strongest Earth tide spectral component M2 was analyzed in time in the aquifer of the Moscow area [54] in terms of its phase shift. Analysis must be restricted to quiet periods, and time windows affected by aquifer inflow fluctuations and other natural and anthropogenic level influences must be excluded from the analysis. The goal of the study is to use the phase shifts of M2 to infer aquifer permeability changes.

Radon concentrations have been ascribed to strain variations. Mentes [55] used Earth tides measurements to test the following hypothesis: all strain components have lunar tidal frequencies, so if strain variations induce Radon variations, these frequencies must be found in its amplitude spectrum. The presence of only solar frequencies in the Radon, showed that the Radon does only depend on temperature and pressure changes, but not on the strain changes, or at least in a negligible proportion.

Nowadays it is widely acknowledged, that geodetic records of geophysical processes frequently exhibit temporal correlation, which should not be ignored when parameters of interest (e.g., seasonal signals or trend) are to be determined. The time-correlated noise signatures in gravity records were investigated with ARMA (autoregressive-moving-average), PL (power-law), and GGM (Generalized Gauss-Markov) model. The obtained optimal stochastic model could be finally be used to infer realistic uncertainties on the long-term drift for instance [56].

2.2. Geodynamics and the earthquake cycle

The correct functioning of the geodetic instrumentation is guaranteed when the Earth tides signal is well observed, and transient signals can then be looked for in the time series. These include the deformation of the earthquake preparation phase, the coseismic, and the postseismic relaxation, the long term tectonic deformation, and the eigenvibrations (normal modes) of the Earth, or equivalently its free oscillations. Instruments useful in this context are tiltmeters, extensometers, broad-band seismometers, gravity meters, and GNSS receivers.

2.2.1. Observations of signals generated by an earthquake

Free oscillations were analyzed for broadband seismometers, extensometers and tiltmeters (BFO observatory, [24]) and different SGs [57] determining well definable activation of the Earth's free oscillations for important earthquakes as the Sumatra-Andaman 2004, the 2011 Tohoku-Oki and the Chile 2010. Zürn [9] compared synthetic signals with observed modes and found that including the local elastic effects (quantified using tides observed by the same instruments) in the synthetics helps to reduce the misfits significantly. These local effects could be responsible for the commonly observed discrepancies between recorded horizontal seismograms and corresponding theoretical ones. Zhang [58] inverted the focal mechanism and moment magnitude from an inversion of the free oscillation spectra of worldwide SGs using the free-share MINEOS software package (https://geodynamics.org/cig/software/mineos/) for calculating the free oscillation eigenfunctions.

Long-term extensometers in California and Nevada have given up to 40 years continuous measurements, over a broad spectrum of frequencies, from quasi-static to seconds. Strain rates are consistently higher near the fault (0.5 microstrain/yr), and decrease with increasing distance, and match strain rates recovered from GPS networks. At sub-daily periods the noise-level of the strainmeters is about 10 000 times lower than the GPS derived strain rate. The instruments located near major faults have observed a number of episodes of rapid strain change over periods from minutes to weeks; in many cases these appear to reflect shallow creep on the fault nearby, but there are also slow-slip episodes on the San Jacinto fault at seismogenic depths: these appear to be triggered by moderate local earthquakes and larger regional ones. In almost 200 instrument-years of data no anomalous strains have been seen before earthquakes [17].

Spectral analysis was applied to investigate the effects of earthquakes and seismic oscillations on crustal deformation recordings of significant ($M > 7$) earthquakes observed by two quartz-tube extensometers and a Earth tidal monitoring gravimeter operating in the Matyashegy Gravity and Geodynamical Observatory, Hungary. These data were compared with a three component STS-2 seismometer operating in the Kövesligethy Radó Seismological Observatory in Budapest, Hungary [59]. Based on the FFT (Fast Fourier Transform) and cross power spectral densities it was concluded that there were many similarities between the spectral components of recorded teleseismic waves and seismic noise for the different types of observations. In the case of the extensometer and the radial component of STS-2, disturbances occurred in the same frequency range for all the investigated earthquakes, and highest amplitudes of FFT spectra (in the frequency range of 30–80 mHz) were mainly at the same frequencies, probably due to the free oscillation of the Earth. The highest cross power spectral densities due to seismic disturbances were obtained typically in the frequency band 0.05–200 mHz (or period range 5 s–6 h).

Postseismic deformation has been modeled for the TIGA GNSS network (GPS Tide Gauge Benchmark Monitoring - Working Group), estimating vertical and horizontal velocities for the GNSS stations for which post-seismic deformation was recorded. Besides the linear velocity, the post-seismic term was added in form of logarithmic and exponential functions models in order to describe the post-seismic decay as a part of the entire time series. A pronounced post-seismic signal was observed for the Tohoku *M*w9.0 undersea megathrust earthquake of March 11, 2011 off the coast of Japan, the Chile *M*w8.8 event of Feb.27,2010, and Peru *M*w8.4 event of June 23.2010, the postseismic signal lasting from 6 to 10 years [60].

The coseismic displacements of the Gorkha, Nepal *M*w7.8 event of April 25, 2015 were seen to be 1.7 m and a few mm over the fault and at 150 km distance from the fault, respectively. The average strain rate over 5 years compared to the coseismic strain release found an estimated 235 yr interval to store the released seismic energy [61].

Transients in GNSS time series observed in islands behind the Ryukyu Arc, between the Arc and the Okinawa subduction trough (Japan) are interpreted as SSE (slow slip events) on thrust faults, since their onset is not associated with an earthquake. The SSEs are found to repeat at biannual period, and are modeled with a fault moving aseismically with an average moment magnitude of *M*w6.6 [62]. Another large slow slip fault extending over a length of 250 km was modeled behind the Izu-Bonin Arc [63], which generates transient eastward movements of the islands. The movement can also be interpreted as an early stage back-arc rifting commencing

behind the northernmost part of the Izu-Bonin Arc. The transients found in GNSS data at the Bonin Islands have been confirmed to be repeating SSEs by an independent geodetic network of VLBI (Very Long Baseline Interferometry) [64]. The transients are described with a logarithmic or exponential function with a similar function as the post seismic deformation, but with much shorter time constant, since the transient lasts only a few weeks or months.

2.2.2. Observation of long term deformation and correction measures for atmospheric effects

An innovative approach to determine the long period signal and the periodicities in ITRF2014 coordinate time series from VLBI, GPS, and DORIS was done by modeling the time series as discrete-time Markov processes. This approach is particularly well suited in case of nonlinearities in the time series [65]. Seasonal periodicities were analyzed for globally distributed GPS stations using the database of time series published by the Nevada Geodetic Laboratory, with the aim of explaining the seasonal components from atmospheric (surface pressure from ERA model), hydrologic (MERRA land model) and ocean non-tidal (ECCO2 ocean bottom pressure model) loadings. Singular Spectrum Analysis [66,67] was applied to determine mutually orthogonal principal components in all the considered time-series. It was found that the Up component of the GPS signal has the greatest correlation to the superposition of annual and semi-annual atmospheric, hydrologic and non-ocean loading, with low correlation for the horizontal GPS components [68,69]. Glacial Isostatic Adjustment is a feature of geodynamics that affects all deformation measurements mentioned above. Steffen et al. [70] calculated stress changes in the deglaciation phase after the last glaciation, and found that glacially induced faults are not limited to Scandinavia, but reach as far south as northern Central Europe [71].

The ongoing uplift in mountain ranges is observed at many orogens using GPS. Braitenberg et al. [19] found that this movement generates a gravity change rate above the noise level of GRACE. They concluded that over the Tibetan plateau the positive residual gravity rate seen from GRACE after correcting for hydrology and glaciers, is compatible with a topographic uplift not mass-balanced by crustal thickening. The crustal thickness has reached the maximum sustainable thickness and reacts with lower crust horizontal mass flow instead of thickening [72].

Seismological and geodetic monitoring was shown to be relevant in geotechnical monitoring of abandoned potash mines 700 m below surface in Germany, that pose hazard due to seismicity, CH_4 gas escape, presence of tectonic faults and roof collapse due to overburden pressure. Successful measures to mitigate the hazard of the abandoned mines are flooding or backfilling of material, and the monitoring demonstrates the decrease of surface subsidence and local seismicity ([73], www.k-utec.de).

Global analysis of the geometry at plate boundaries suggests a westerly polarized flow of lithospheric plates with respect to the underlying mantle. This movement determines asymmetry along subduction arcs, orogens, and rift zones [74,75]. The variations in viscosity at the base of the lithosphere control variations in plate velocity, and are sufficiently low to maintain decoupling of the lithosphere from the underlying mantle [76]. Consequently the solid Earth tide affects the geodynamics and the seismic activity. The horizontal component is westerly polarized due to the misalignment of the Earth's bulge, which may translate in shear stress on the lithosphere and loading of faults [75].

2.3. Variations in Earth rotation

The long term signal of the ring laser gyroscope installed at the geodetic station Wettzell, Germany is to monitor high frequency variations in polar motion and UT1, with special emphasis on non-harmonic geophysical signals [77]. The presentation of Tercjak et al. [78] aimed at modeling the effect of tilt and horizontal displacements induced by Earth and loading tides, non-tidal atmospheric and hydrology loading effects on the ring laser.

LOD (Length of day), and the pole coordinates were investigated by Nastula et al. [79] using GPS and GLONASS observations. The purpose of the study is to investigate the potential of GNSS observations, and in particular those from Galileo for determination of Earth Rotation Parameters at short, down to sub daily, periods.

A high-frequency model of variations in Earth rotation was developed by Hagedoorn et al. [80] based on a new empirical ocean tide model, which should bear an improvement with respect to the IERS 2010 model based on Ray et al. [81]. The ocean tidal angular momenta were calculated and the related short-period variations in Earth rotation were estimated. The cause of the perturbation of LOD (length of day) at the principal diurnal frequency of the solar S1 tide was investigated by [82]. The S1 perturbation observed by VLBI is largely explained by oceanic and atmospheric excitation. The study suggests that variations in the excitation are to be expected by the El Niño Southern Oscillation, which is equivalent in strength to a strong climate perturbation.

Predicting variations in Earth Orientation Parameters is necessary for interplanetary spaceflight missions. The prediction is the sum of a stochastic behavior and a deterministic part, as the tides of the solid Earth and ocean. Gross [83] evaluated the recent tidal models to predict Earth Orientation Parameters in combination with a Kalman filter.

2.4. Tides in space geodetic observations

The presentation open to the public held by H. Schuh [84] illustrated the important role of modern geodesy in the definition and realization of precise and stable geodetic reference frames, required for monitoring changes on the Earth such as plate tectonics or global sea level rise. An overview of the various natural hazards and global change phenomena that can be observed by geodetic techniques was given. Depending on the spatial scale, various types of measurements were illustrated, from space geodetic techniques such as GNSS (Global Navigation Satellite Systems), SLR (Satellite Laser Ranging), VLBI (Very Long Baseline Interferometry), and DORIS (Doppler Orbitography and Radiopositioning Integrated by Satellite), via dedicated gravity satellite missions and regional observations such as airborne gravimetry, to local measurements by geodetic surveying instruments. All these techniques and the underlying models are combined in GGOS, the Global Geodetic Observing System of the IAG, and the concept of this integrative enterprise was described. Case studies were presented that documented the essential role of precise geodetic data, accurate analysis methods, and realistic mathematical and physical models. Examples were the major earthquakes of recent years (Tohoku-Oki 2011, Chile 2014), the volcanic eruption of Eyjafjallajökull on Iceland (2010) and the manifestations of climate change, as sea level and sea temperature change and atmospheric currents.

A second public presentation was held by J. Freymueller [85] on the identification of large amplitude surface loading signals and large tectonic signals of Southern Alaska. As in the presentation by Heki et al. [86] Slow Slip Events (SSE) were identified in GPS displacements on top of the subduction of the Alaska-Aleutian megathrust. These signals have been separated from secular surface mass variations caused by the melting of glacier ice and from seasonal surface mass variations which are caused by snow accumulation and melt. They found that to first order, much of the seasonal deformation can be removed using surface load models based on GRACE observations of gravity change, although there can be differences depending on whether seasonal average or time series

mass loading deformation is removed. In addition, in some places the GRACE signal is smoothed over too large an area to provide a fully accurate correction for GPS position time series.

The long-wavelength mass change within the Earth system, in particular, the Earth's dynamical oblateness characterized by the second degree gravitational zonal geopotential spherical harmonic J2, can be recovered by SLR. The time series of J2 is available over a 40 years period (Cheng and Ries [87,88]). The presentation of Cheng [89] focused on the amplitude and phase and nature of the 18.6-yr variation, which is a wavelength belonging to the tide variations in the solid Earth and ocean. The study showed that effects of mantle inelasticity must be considered when modeling the J2 response to this tidal component.

EOP parameters derived from VLBI and global GNSS have an improved agreement after treating the VLBI data with a Kalman filter, respect to traditional methods. The new method in analyzing the data, opens new prospects for high frequency signal investigations in EOP by VLBI (Karbon et al. [90]).

2.5. Volcano geodesy

The monitoring of volcanoes aims at catching premonitory signals of an eruption and recording the time evolution of a volcano to detect any changes that could indicate an inflation of the edifice and upward mass movement in the volcano conduit. The monitoring includes any type of geodetic measurement of the shape and the continuous gravity measurement.

The Canary Islands are volcanic islands off shore West Africa; the active seismicity demonstrates the subsurface volcanic mass movements. Fernandez et al. [91], adopted Differential Synthetic Aperture Radar images from satellites combined with GNSS monitoring for recording active deformation of several of the Canary Islands. They found that C-band SAR data from ERS/ENVISAT satellites gave good agreement with GNSS vertical and horizontal movement rates.

The highest point in Europe is on the Elbrus volcano in the Caucasian Mountains, a dormant volcano with historical eruptions in Holocene. Here Milyukov et al. [21], measure strain rate through a laser strain-meter, and interpreted resonant frequencies as due to a resonance of the underlying magma chamber. The resonances are observed at the passage of seismic waves generated at near earthquakes (distance up to 500 km) as amplifications at well-defined frequencies. A seismic sounding experiment was accomplished from the center of the volcano outwards along its slope, revealing that a magma chamber is present, and is discernible through a measurable decrease of seismic wave velocities, down to the base of the crust.

The Campi Flegrei caldera is close to the city of Naples (Italy), and has alternating episodes of uplift and subsidence going back to historical times. The last eruption dates to 1538, followed by a general subsidence for 400 years, followed by several uplift episodes superposed on the continuing subsidence. The area of Campi Flegerei has been monitored since 1905 first by a leveling line, then extended successively by an increase of leveling reference points, distance and angular measurements, tiltmeters, and continuous GNSS. The interpretation of the source generating the vertical movement is an important discussion point. Crescentini and Amoruso [92] propose a pressurized finite thin triaxial ellipsoid embedded in a layered medium at about 4 km to model the regional deformation. Residual smaller scale deformation not accounted for by this source is explained by a small (point) pressurized oblate spheroid about 2 km below the surface and laterally displaced with respect to the deeper source. The location and geometry of the two sources are constant in time, with the exception of volume changes (potency); potency time histories are somewhat similar but not identical. Most recent GNSS and SAR data confirm this model, initially proposed by Amoruso et al. [93,94].

2.6. Natural and anthropogenic subsurface fluid effects

Geodetic measurements are influenced by the hydrosphere: we must distinguish the mass change, sensed directly by the gravity field and observation of Earth deformation, originated by elastic yielding to the load change. Further the subsurface hydrology induces deformation through pore pressure changes in a porous media or leads to pressure changes in the aquifer due to the hydraulic head. This effect is particularly strong in karstic environs, where the flow is restricted to channel conduits in which pressure builds up to several atmospheres after rainfall. These hydrologic flows can be natural or man-made, according to the source of the water masses. An important issue is whether the pressure changes induced by the hydrology are responsible for induced seismicity, be it natural or man-made. The geodetic measurements that sense the hydrologic effects include observations of gravity and deformation.

Absolute gravity measurements made 10 m below the surface compared to continuous surface gravity measurements made with a spring gravimeter in Riga (Latvia) demonstrated a seasonal gravity change differences of up to 16 microgal (peak to peak) that is ascribed to soil moisture changes, with an excellent correlation to the water-table yearly variations of 0.5 m (peak to peak), Mäkinen et al. [95]. Two SGs were set side by side at 3 m distance at Metsähovi station (Finland), and differences up to 20 microGals were found, not ascribable to instrumental errors. The differences are due to transient hydrological movement after heavy precipitation (Virtanen and Raja-Halli [14]).

The SGs are the ideal stationary instruments for monitoring hydrologic mass changes due to their high sensitivity and low drift rate. In northern Benin (West-Africa, Djougou) Calvo et al. [36] illustrated six years of SG observations and the correlation to water table depth and precipitation. They find that the atmospheric tidal S1 and S2 pressure signal is strong in this subtropical region.

A network of repeated microgravity measurements combined with a continuous reference gravity station, controlled by regular co-located absolute gravity measurements is the strategy planned by Hinderer et al. [96] to monitor gravity changes associated to geothermal activity. The experimental sites are associated with two geothermal reservoirs in northern Alsace, where geothermal energy is used either for industrial purposes or for producing electricity. The modeling of gravity and surface changes is done taking into account both attraction and elastic deformation effects.

Over-exploitation of an aquifer leads to loss of the aquifer storage due to compaction and land subsidence. Abajo et al. [97] analyzed the Lorca area in Spain, which has the Europe-wide highest aquifer-related subsidence (>10 cm/yr) [98], by differential radar interferometry. Apart from the subsidence, the subsurface stress field is altered close to an active seismogenic source, which poses the question whether the prolonged water extraction has altered the seismic hazard.

The hydrologic signal in two separated karst systems 110 km apart was analyzed through tilt and GNSS by Braitenberg et al. [99] and Grillo et al. [20]. The 50 years long observations of the ultra broad band Marussi horizontal pendulums Braitenberg et al. [100] showed that the tilt signal is proportional to the integrated volume of the water flow entering the Karst plateau (Tenze et al. [101]), and flowing in conduits at a couple of 100 m below the topographic surface. The hydrologic signal is prominent in tilt, and should produce also a signal in the continuous GNSS due to the expected displacement induced by pressure in the karstic flow conduits. The research shows that the well identified hydrologic deformations in tilt can be useful as a guide for distinguishing analogous signals in the GNSS, which are less evident, because the signal to noise ratio on GNSS is order of magnitudes smaller than the one of the underground tilt signal. The local hydrologic displacement above

Grotta Gigante recorded by GNSS is up to 8 mm, affecting both horizontal and vertical components, with an upward movement during a flood. The tilt signal is up to 0.6 μrad, with consistent tilt and displacement directions. In the Genziana station, Italy, (the Cansiglio karstic plateau to the north-west of the Trieste Karst), the hydrologic signal has ten-fold amplitude, and correlates very well with the local karstic springs [20]. The 50 year long observations show a long term NE-ward tilting of 0.1 nrad/day, with 31 year period modulation, confirming the wavelength identified a decade ago (Braitenberg et al. [102]).

The intrinsic variability of the long-term tilting, which includes the solar yearly period, poses a restriction on the minimum time window size useful to determine the long-term linear tilting rate. Increasing successively the analysis window for the linear regression of the tilt rate from 5 years to 50 years, the rate varies over a range of 0.3 nrad/day and remains stable at the value of 0.1 nrad/day for time windows between 30 and 50 years long. The result shows that a deformation rate calculated over 5–30 years does not represent the long-term stable trend, but is an instantaneous deformation rate. At least 30 years of observation are necessary to determine the long term deformation rate due to the yearly and hydrologic signals. It can be assumed that for GNSS observations similar time windows are necessary before the stable movement rate can be determined, in particular in stations affected by an observable yearly movement.

Using a network of GNSS stations that extends in NE-Italy over a length of 150 km and comprises the above mentioned two karstic areas, the time series were analyzed in terms of their trend and frequency content. An apparent transient signal of about 2-year period was identified, which was ascribed to a porosity wave, originated by fluid mobilization due to tectonic processes in the area (Rossi et al. [103]). The results were further analyzed in terms of porosity and pore-pressure at depth successively (Rossi et al. [104]).

In an effort to correct GNSS observations for hydrologic effects Boy [105], was concerned with the GLDAS (Global Land Data Assimilation System) soil moisture model lacking groundwater and surface water components. Surface water storage was derived from river water elevation estimates, which was used as proxy for runoff outputs from a hydrologic model. The river water height was inferred from the river width, which can be derived from MODIS (Moderate Resolution Imaging Spectroradiometer) remote sensing images. The entire continental water storage, sum of soil-moisture, snow and modeled surface water, is found to better explain GNSS surface displacements and is in better agreement with GRACE, compared to the GLDAS model.

The Geodynamic Observatory Moxa in Thuringia, Germany houses strain and tilt meters, gravimeters installed starting from 1990, and is fully equipped with environmental monitoring stations, with time series over 15 year long. These include snow, soil moisture and water table observations. The correlation between induced deformation and environmental parameters was found in many cases. The order of magnitude of a transient strain after strong rain fall is 300 nstrain on the strainmeter, with 40 mm groundwater transient rise, and very similar time evolution among the two quantities (Jahr [22]). The interpretation of the SG of Moxa requires detailed modeling of the soil moisture, hydrology, snow cover, integrated in a high resolution digital terrain model of the building, the soil above its roof and the terrain (Weise and Jahr [23]). The correction of the SG time series with the above parameters improves correlation to GRACE. The study demonstrates that GRACE cannot be used to correct the geodetic observations for hydrologic effects, since the local influence can be preponderant. Further the GRACE signal is a low pass filtered version of the existing gravity changes, with a cut off filter wavelength of at least 330 km (assuming $N = 120$ as the maximum observed degree in the spherical harmonic expansion).

2.7. Instruments and software developments

Innovations in instrumentation and software are important for the researchers working on the data as well as for the innovation of existing laboratories. The presentations ranged from gravity meter developments including atom interferometric gravimeter, the efforts in China to build a new GOCE-type satellite, to the interferometric fluid level tiltmeter, to software innovations in acquiring and analyzing geodetic data.

A modern version of the interferometric Michelson-Gale (M-G) type water level tilt meter (named NSiWT, 50.4 m length) has been developed and built at the Finnish Geodetic Institute (FGI) in 2000–2007. The tiltmeter has been recording continuously in Lohja2 geodynamic station (Tytyri mine), Lohja, Finland since 2008 (Ruotsalainen [106]). The Fizeau-Kukkamäki type level interferometers guarantee stable internal scale [12,13]. Thermal expansion and eigenfrequency of the instrument have been modelled for suitable physical conditions at the recording site by (Ruotsalainen [107]). Primary research goal is to validate ocean tide loading models from the Baltic Sea and atmospheric tilt loading models through NSiWT tilt observations for high precision geodesy and Earth modeling. Recently a new M-G type one end prototype tilt meter with 5.5 m length, was built at the FGI in cooperation with the Geodetic and Geophysical Institute (GGI), Hungarian Academy of Sciences (HAS), Sopron, Hungary (owner of the instrument). The M-G type prototype tilt meter (named W_iWT) was installed 2014 in cooperation with GGI in the Conrad geophysical observatory, which is operated by the Central Institute for Meteorology and Geodynamics, Austria (Ruotsalainen et al. [16,108]). First results from comparison with a parallel recording Lippman type 2D tilt meter of the GGI (HAS) are promising (Ruotsalainen et al. [108]). Effects of water extraction from wells were observed on a laser strainmeter in Moscow, where weekly cycles were observed reflecting water consumption habits of the population (Volkov et al. [109]). Atmospheric pressure systems as those that arise with tropical cyclones were analyzed in terms of deformations in strainmeters and tiltmeters. The possible effect of the loading on microsesimicity was also analyzed (Volkov et al. [110]).

The Geodynamic Observatory Moxa has continuous tilt, extensometric and gravity monitoring instrumentation. The unequivocal effect of a pressure wave induced by injection or extraction during a drilling experiment into a borehole placed not far from the observatory was discussed by Jahr [22] showing the correlated signals found in the strain instruments compared to the groundwater changes. The compressional wave induced a transient compression on strain, and uplift of the soil above the borehole, with consequent tilting of the surface away from the borehole. Both the signals were well seen on the tilt and strainmeters, with reverse effects observed when water was extracted in the borehole.

The automated Burris gravimeter was discussed and its properties in terms of resolution, repeatability, and drift rate (Jentzsch et al. [111]) was analyzed. The resolution in continuous reading mode is 0.0001 mGal, with a worldwide measuring range of 7000 mGal, and drift is approximatly 1 mGal/month for a new instrument, lowering to less than 0.3mGal/month for a mature system. Earth tides and free oscillations generated by a major earthquake were shown to be reliably measured. A new control software installed on a portable PC integrates the gravimeter control and data acquisition with data from a pressure gauge and a GPS sensor. A further improvement concerns the feedback control-system of the gravimeter, which results in an overall better instrumental performance in terms of accuracy. The new software is also capable of making the tidal and drift corrections and importing the terrain gravity effect for the observation stations (Schulz et al. [112]). A few studies were concerned with the calibration of superconducting gravimeters through

common location of instruments as vertical seismometers (Luo and Xu [113]), absolute gravity meters (Crossley et al. [114]), and the critical review of the step response method for the empirical determination of the transfer function by relative comparison of collocated superconducting gravimeters (Wziontek [115]). Significant discrepancies were found which could not be confirmed by cross-correlation of the regular signal, demonstrating that the applied method may disturb the system, depending on the initialization of the sensor. The topics are technical and concern the detailed construction of the SGs, the properties of the internal filter, the feedback system and their frequency transfer function.

A useful software for the treatment of time series observations from a geodetic instrument is the PreAnalyseExtended, a graphical user software useful for the data screening, management and analysis of general data acquired from geophysical instrumentation by Gebauer [116]. Tools include interpolation of data-gaps, data steps and spike handling, data calibration, filtering, detrending and geophysical modeling as tidal modeling and Sagnac-frequency modeling for the ring-laser. Tools for data management, including log book and visualization, are included. The software is platform-independent and can be enriched with user-written data-analysis modules.

An innovative service for continuous geodetic monitoring consists in installing single-frequency GNSS receivers, which are analyzed with the free and open software goGPS, and providing a dedicated monitoring unit (Geoguard). The goGPS implements an extended Kalman filter, with GNSS code and phase observations as input (Caldera et al. [117]). The displacements are retrieved at mm-level (Sampietro et al. [118]).

3. Conclusions

The International Symposium on Geodynamics and Earth Tides is an interdisciplinary gathering of researchers discussing on all aspects that affect high precision geodetic monitoring. The one-session structure allows maximum discussion, and a relatively large audience of over 100 international specialists. The scientific innovations are distributed between instrumentation, the experimental proof of theoretically predicted signals, and methodological innovations. The studied phenomena are all dynamic, which requires continuous monitoring of the particular signals and the time-lapse study of the observed time-series. Many of the investigated topics are relevant to the well-being of modern society, that is vulnerable to hazards posed by earthquakes, volcanism, subsidence or inflation, Earth rotation changes, climatic changes and by hazards due to mining, induced seismicity, land-slides. The 18th International Symposium on Geodynamics and Earth Tides demonstrated the general relevance of these topics and the importance to increment the diffusion and awareness of the globally distributed monitoring stations.

Useful links

IGETS terms of reference: http://igets.u-strasbg.fr/Documents/IGETS_ToR.pdf.

IGETS, 2017: http://igets.u-strasbg.fr/index.php.

IGETS database, 2017: http://isdc.gfz-potsdam.de/igets-database/.

BIM Earth Tides Bulletin: http://www.bim-icet.org/.

GNSS cost-effective monitoring: http://www.gogps-project.org/, http://www.geoguard.eu/.

Ocean loading [41]: https://igppweb.ucsd.edu/~agnew/Spotl/spotlmain.html.

TIGA-GNSS network: http://adsc.gfz-potsdam.de/tiga/.

Wettzell Observatory, Germany: https://www.bkg.bund.de/EN/Home/home.html.

Acknowledgements

The Symposium was scientifically supported by the IAG: Commission 3, the IAG Sub-commission 3.1 and International Geodynamics and Earth Tide Service. The University of Trieste and the sponsors of the Symposium, namely the OGS (Istituto Nazionale di Oceanografia e di Geofisica Sperimentale), the Dipartimento di Fisica E. Caianiello, University of Salerno, the Department of Mathematics and Geosciences of the University of Trieste, Leica Geosystems S.P.A., International Association of Geodesy (3 IAG Travel Awards for young scientists), the European Geosciences Union (support to 8 young scientists), the Rector Maurizio Fermeglia of the University of Trieste and the President Maria Cristina Pedicchio of OGS, Institute of oceanography and applied geophysics are gratefully acknowledged for supporting this event.

The following colleagues are thanked for constructive comments: J. Bogusz., L. Crescentini, K. Heki, J. Hinderer, G. Jentzsch, G. Mentes, G. Papp, S. Rosat, G. Rossi, H. Ruotsalainen, H. Schuh, W. Zürn. D. Crossley is thanked for review of the manuscript. Dr. I. Nagy is thanked for assistance in retrieving references.

Part of the research is realized through the contribution of the Italian Space Agency in the frame of the project “MOCASS” (- Mass Observation with Cold Atom Sensors in Space. The maps were created using the GMT (Generic Mapping Tools) software package [119].

Appendix A. Abstracts

The abstracts collection of this symposium can be found at https://doi.org/10.1016/j.geog.2018.03.003.

References

[1] H. Drewes, Geodesist's handbook 2008, J. Geod. 82 (2008) 661–846, https://doi.org/10.1007/s00190-008-0259-0.
[2] H. Drewes, The Geodesist's handbook 2012, J. Geod. 86 (2012) 793–974.
[3] H. Drewes, The Geodesist's handbook 2016, J. Geod. 90 (2016) 911–1205.
[4] IGETS (International Geodynamics and Earth Tide Service), http://igets.u-strasbg.fr/index.php. (Accessed 28 December 2017).
[5] A. Amoruso, L. Crescentini, Nonlinear and minor ocean tides in the Bay of Biscay from the strain tides observed by two geodetic laser strainmeters at Canfranc (Spain), J. Geophys. Res. Oceans 121 (2016) 4873–4887, https://doi.org/10.1002/2016JC011733.
[6] A. Amoruso, L. Crescentini, A. Bayo, S. Fernández Royo, A. Luongo, Two high-sensitivity laser strainmeters installed in the Canfranc underground laboratory (Spain): instrument features from 100 to 0.001 mHz, Pure Appl. Geophys. (2017), https://doi.org/10.1007/s00024-017-1553-7.
[7] S. Rosat, S. Lambotte, U. Riccardi, J.P. Boy, F. Boudin, W. Zürn, Tidal Analyses of Long-base Tiltmeters at Rustrel (France), Sainte-Croix (France) and BFO (Germany), Geodesy Geodyn. 9 (3) (2018).
[8] F. Boudin, P. Bernard, L. Longuevergne, N. Florsch, C. Larmat, C. Courteille, et al., A silica long base tiltmeter with high stability and resolution, Rev. Sci. Instrum. 79 (2008) 034502, https://doi.org/10.1063/1.2829989.
[9] W. Zürn, Local Elastic Effects in Low-Frequency Spectra of Earth's Free Oscillations, Geodesy Geodyn. 9 (3) (2018).
[10] H. Otto, H.-G. Wenzel, K.H. Zahran, W. Zürn, Tidal analysis of DFP-tiltmeter observations 1993 – 1996 at the Black Forest Observatory (BFO), in: B. Ducarme, P. Paquet (Eds.), Proc. 13th Int. Symp. Earth Tides. Obs. R. de Belgique, Brussels, 1998, pp. 141–148.
[11] A.M.G. Ferreira, N.F. D'oreye, J.H. Woodhouse, W. Zürn, Comparison of fluid tiltmeter data with long-period seismograms: surface waves and Earth's free oscillations, J. Geophys. Res. 111 (2006), https://doi.org/10.1029/2006JB004311.
[12] H. Ruotsalainen, Interferometric water level tilt meter development in Finland and comparison with combined earth tide and ocean loading models, Pure Appl. Geophys. (2017), https://doi.org/10.1007/s00024-017-1562-6.
[13] H. Ruotsalainen, M. Nordman, J. Virtanen, H. Virtanen, Ocean tide, Baltic Sea and atmospheric loading model tilt comparisons with interferometric geodynamic tilt observation – case study at Lohja2 geodynamic station, Southern Finland, J. Geod. Sci. 5 (2015), https://doi.org/10.1515/jogs-2015-0015.
[14] H. Virtanen, A. Raja-Halli, Parallel observations with three superconducting gravity sensors during 2014–2015 at Metsähovi geodetic research station, Finland, Pure Appl. Geophys. (2017), https://doi.org/10.1007/s00024-017-1719-3.
[15] A. Weise, G. Jentzsch, J. Kääriäinen, A. Kiviniemi, H. Ruotsalainen, Tilt Measurements in Geodynamics – Results from the 3-component-station Metsähovi and the Clinometric Station Lohja/Finland, in: H.-T. Hsu (Ed.), Proc

12th Int Symp Earth Tides Beijing Aug 4-7, 1993, Science Press, Beijing, 1995, pp. 105–114.
[16] H. Ruotsalainen, D. Bán, G. Papp, R. Leonhardt, J. Benedek, Interferometric Water Level Tilt Meter at the Conrad Observatory. COBS J. Sci. Contrib. 2014 – 2015. Conrad observatory, Zentralanstalt für Meteorologie und Geodynamik, eine Forschungseinrichtung des Bundesministerium für Wissenschaft, Forschung und Wirtschaft, Austria, 2016.
[17] D. Agnew, F. Wyatt, Long-Base Laser Strainmeters: four Decades of Results, G-ET2016, Geodesy Geodyn. 9 (3) (2018).
[18] M. Kaczorowski, Z. Szczerbowski, D. Kasza, R. Zdunek, M. Jozwik, R. Wronowski, Investigation of Relationships in Time-Domain Between Tectonic and Tidal Signals Observed in the Geodynamic Laboratory of SRC and Seismic Events Which Occur in the Middle Odra Faults Zone (The Lower Silesian Copper Mining Region), Geodesy Geodyn. 9 (3) (2018).
[19] C. Braitenberg, T. Pivetta, W. Chen, E. Serpelloni, Interference of Tectonic Signals in Subsurface Hydrologic Monitoring Through Gravity and GNSS due to Mountain Building, Geodesy Geodyn. 9 (3) (2018).
[20] B. Grillo, C. Braitenberg, I. Nagy, R. Devoti, D. Zuliani, P. Fabris, Cansiglio karst-plateau: ten years of geodetical-hydrological observations in seismically active North-east Italy, Pure Appl. Geophys. (2018), https://doi.org/10.1007/s00024-018-1860-7.
[21] V. Milyukov, E. Rogozhin, A. Gorbatikov, A. Mironov, A. Myasnikov, M. Stepanova, Contemporary state of the Elbrus volcanic center (The Northern Caucasus), Pure Appl. Geophys. (2017), https://doi.org/10.1007/s00024-017-1595-x.
[22] T. Jahr, Non-tidal tilt and strain signals recorded at the Geodynamic Observatory Moxa, Thuringia/Germany, Geod. Geodyn. 9 (2018) 229–236.
[23] A. Weise, T. Jahr, The improved hydrological gravity model for Moxa observatory, Germany, Pure Appl. Geophys. (2017), https://doi.org/10.1007/s00024-017-1546-6.
[24] D. Bán, G. Mentes, M. Kis, A. Koppán, Observation of the earth liquid core resonance by extensometers, Pure Appl. Geophys. (2017), https://doi.org/10.1007/s00024-017-1724-6.
[25] G. Mentes, Quartz tube extensometer for observation of Earth tides and local tectonic deformations at the Sopronbánfalva Geodynamic Observatory, Hungary, Rev. Sci. Instrum. 81 (2010) 074501, https://doi.org/10.1063/1.3470100.
[26] I. Eper-Pápai, G. Mentes, M. Kis, A. Koppán, Comparison of two extensometric stations in Hungary, J. Geodyn. 80 (2014) 3–11, https://doi.org/10.1016/j.jog.2014.02.007.
[27] G. Mentes, Z. Berta, First results of the extensometric measurements in South Hungary, Bull D'Inf Marées Terr 127 (1997) 9744–9749.
[28] L. Brimich, M. Bednarik, P. Vajda, D. Bán, I. Eper-Pápai, G. Mentes, Extensometric Observation of Earth Tides and Local Tectonic Processes at the Vyhne Station, Slovakia, Geodesy Geodyn. 9 (3) (2018).
[29] L. Brimich, M. Bednárik, V. Bezák, I. Kohút, D. Bán, I. Eper-Pápai, et al., Extensometric observation of Earth tides and local tectonic processes at the Vyhne station, Slovakia, Contrib. Geophys. Geod. 46 (2016), https://doi.org/10.1515/congeo-2016-0006.
[30] P. Varga, E. Grafarend, J. Engels, Relation of different type Love-Shida numbers determined with the use of time-varying incremental gravitational potential, Pure Appl. Geophys. (2017), https://doi.org/10.1007/s00024-017-1532-z.
[31] P. Varga, E. Grafarend, Influence of tidal forces on the triggering of seismic events, Pure Appl. Geophys. (2017), https://doi.org/10.1007/s00024-017-1563-5.
[32] J. Petersen, Observations and Modelling of Background Seismic Noise. Open-file Report 93–322, U. S, Geological Survey, Albuquerque, New Mexico., 1993, pp. 1–42.
[33] S. Rosat, J. Hinderer, J.P. Boy, F. Littel, D. Boyer, J.-D. Bernard, et al., First Analyses of the New iOSG-type Superconducting Gravimeters at the J9 Gravimetric Observatory of Strasbourg and at the Low Noise Underground Laboratory of Rustrel, France, Geodesy Geodyn. 9 (3) (2018).
[34] B. Meurers, M. Van Camp, O. Francis, V. Pálinkáš, M2 Tidal Parameter Modulation Revealed by Superconducting Gravimeter, Geodesy Geodyn. 9 (3) (2018).
[35] B. Meurers, Scintrex CG5 used for superconducting gravimeter calibration, Geod. Geodyn. 9 (2018) 197–203.
[36] M. Calvo, H. Basile, J.P. Boy, J. Hinderer, S. Rosat, F. Littel, et al., The Djougou (Benin, West Africa) Permanent Superconducting Gravity Station: 2010 – 2016, Geodesy Geodyn. 9 (3) (2018).
[37] D. Crossley, T. Murphy, Processing SG Data According to the Requirements of the IGETS Database, with Apache Point as an Example, Geodesy Geodyn. 9 (3) (2018).
[38] H. Wziontek, R. Falk, K. Schüller, S. Zerbini, 18 Years Continuous Gravity Time Series at Station Medicina: a Benchmark For Tidal Analysis, Geodesy Geodyn. 9 (3) (2018).
[39] N. Lesparre, F. Boudin, C. Champollion, J. Chéry, C. Danquigny, H.C. Seat, et al., New insights on fractures deformation from tiltmeter data measured inside the Fontaine de Vaucluse karst system, Geophys. J. Int. 208 (2017) 1389–1402, https://doi.org/10.1093/gji/ggw446.
[40] F.A. Oreiro, H. Wziontek, M.M.E. Fiore, E.E. D'Onofrio, C. Brunini, Non-tidal Ocean loading correction for the Argentinean-German geodetic observatory using an empirical model of storm surge for the Río de la Plata, Pure Appl. Geophys. (2017) 1–15, https://doi.org/10.1007/s00024-017-1651-6.
[41] D.C. Agnew, SPOTL: Some Programs for Ocean-Tide Loading, SIO Technical Report, Scripps Institution of Oceanography (2012) 1–45. https://escholarship.org/uc/item/954322pg. (Accessed 3 April 2018).
[42] P.-M. Rouleau, On GPS-based Ocean Tidal Loading Displacements and Their Potential to Constrain Mechanisms of Anelasticity, Geodesy Geodyn. 9 (3) (2018).
[43] J.P. Boy, P. Baudet, A. Mémin, P. Ulrich, Validation of EOST Loading Service Using Global GPS Solutions, Geodesy Geodyn. 9 (3) (2018).
[44] M. Rodell, P.R. Houser, U. Jambor, J. Gottschalck, K. Mitchell, C.-J. Meng, et al., The global land data assimilation system, Bull. Am. Meteorol. Soc. 85 (2004) 381–394, https://doi.org/10.1175/BAMS-85-3-381.
[45] K.H. Zahran, J. Hinderer, E. Issawy, J.-P. Boy, S. Rosat, M. Taweel, et al., New Gravimetric Tide Observations in the Vicinity of Lake Nasser, Geodesy Geodyn. 9 (3) (2018).
[46] G. Papp, L. Battha, F. Bánfi, CCD ocular system for the LaCoste and Romberg G meters (in Hungarian with English abstract), Publ. Geomat. 12 (2009) 83–90.
[47] G. Papp, J. Benedek, P. Varga, M. Kis, A. Koppán, B. Meurers, R. Leonhardt, M.K. Baracza, Feasibility study applied to mapping tidal effects in the Pannonian basin – an effort to check location dependencies at μGal level, Geod. Geodyn. 9 (2018) 237–245.
[48] G. Papp, E. Szűcs, L. Battha, Preliminary analysis of the connection between ocean dynamics and the noise of gravity tide observed at the Sopronbánfalva Geodynamical Observatory, Hungary, J. Geodyn. 61 (2012) 47–56, https://doi.org/10.1016/j.jog.2012.07.004.
[49] M. Kis, A. Koppán, L. Merényi, G. Papp, J. Benedek, E. Szűcs, B. Meurers, Moving-mass calibration of LCR-G gravimeters- Determination of Beam-position Dependent Transfer Functions in the Mátyáshegy Gravity and Geodynamical Observatory, Budapest, Geodesy Geodyn. 9 (3) (2018).
[50] S. Rosat, B. Escot, J. Hinderer, J.-P. Boy, Analyses of a 426-day record of seafloor gravity and pressure time series in the North Sea, Pure Appl. Geophys. (2017), https://doi.org/10.1007/s00024-017-1554-6.
[51] L. Besutiu, Non-tidal Gravity Change and Vrancea Intermediate-Depth Seismicity, Geodesy Geodyn. 9 (3) (2018).
[52] J. Xu, Q. He, X. Chen, J. Zhou, H. Sun, Long-term Gravity Changes in Lhasa, Tibet and Their Implication to Hydrology and Crust Movement, Geodesy Geodyn. 9 (3) (2018).
[53] D.C. Agnew, An improbable observation of the diurnal core resonance, Pure Appl. Geophys. (2017), https://doi.org/10.1007/s00024-017-1522-1.
[54] E. Vinogradov, E. Gorbunova, A. Besedina, N. Kabychenko, Earth tide analysis specifics in case of unstable aquifer regime, Pure Appl. Geophys. (2017), https://doi.org/10.1007/s00024-017-1585-z.
[55] G. Mentes, Investigation of the Relationship Between Rock Strain and Radon Concentration in the Tidal Frequency Domain, Geodesy Geodyn. 9 (3) (2018).
[56] J. Bogusz, S. Rosat, A. Klos, J.-P. Boy, Time-correlated Noise Signatures in Gravity Records, Geodesy Geodyn. 9 (3) (2018).
[57] M. Abd El-Gelil, M. Al-Shahri, Observation of Earth Free Oscillation Modes Using Cross Least Squares Wavelet Method, Geodesy Geodyn. 9 (3) (2018).
[58] L. Zhang, Constrain Large Earthquake Source Mechanism by Using Low Frequency Normal Mode Data, Geodesy Geodyn. 9 (3) (2018).
[59] M. Kis, A. Koppán, G. Mentes, D. Bán, M. Kiszely, K. Gribovszky, et al., Analysis of Effects Related to Earthquakes and Seismic Oscillations Appearing in Rock Deformation and Gravimeter Recordings, Geodesy Geodyn. 9 (3) (2018).
[60] A. Klos, M. Gruszczynska, M.S. Bos, J.-P. Boy, J. Bogusz, Estimates of vertical velocity errors for IGS ITRF2014 stations by applying the improved singular spectrum analysis method and environmental loading models, Pure Appl. Geophys. (2017), https://doi.org/10.1007/s00024-017-1494-1.
[61] F. Morsut, T. Pivetta, C. Braitenberg, G. Poretti, Strain accumulation and release of the Gorkha, Nepal, earthquake (*Mw*7.8, 25 April 2015), Pure Appl. Geophys. (2017), https://doi.org/10.1007/s00024-017-1639-2.
[62] Y. Tu, K. Heki, Decadal modulation of repeating slow slip event activity in the southwestern Ryukyu Arc possibly driven by rifting episodes at the Okinawa trough: decadal modulation of SSE activity, Geophys. Res. Lett. 44 (2017) 9308–9313, https://doi.org/10.1002/2017GL074455.
[63] D. Arisa, K. Heki, Transient crustal movement in the northern Izu–Bonin arc starting in 2004: a large slow slip event or a slow back-arc rifting event? Tectonophysics 682 (2016) 206–213, https://doi.org/10.1016/j.tecto.2016.05.029.
[64] D. Arisa, K. Heki, Space geodetic observations of repeating slow slip events beneath the Bonin Islands, Geophys. J. Int. 210 (2017) 1494–1502, https://doi.org/10.1093/gji/ggx258.
[65] V. Tornatore, E. Tanır Kayıkçı, M. Roggero, Comparison of ITRF2014 station coordinate input time series of DORIS, VLBI and GNSS, Adv. Space Res. 58 (2016) 2742–2757, https://doi.org/10.1016/j.asr.2016.07.016.
[66] D.S. Broomhead, G.P. King, Extracting qualitative dynamics from experimental data, Phys. Nonlinear Phenom. 20 (1986) 217–236, https://doi.org/10.1016/0167-2789(86)90031-X.
[67] R. Vautard, M. Ghil, Singular spectrum analysis in nonlinear dynamics, with applications to paleoclimatic time series, Phys. Nonlinear Phenom. 35 (1989) 395–424, https://doi.org/10.1016/0167-2789(89)90077-8.
[68] M. Gruszczynska, A. Klos, M.S. Bos, J.-P. Boy, J. Bogusz, Assessing the Seasonal Signals Between Environmental Loadings and GPS Coordinates With Singular Spectrum Analysis, Geodesy Geodyn. 9 (3) (2018).
[69] A. Klos, M. Gruszczynska, M.S. Bos, J.-P. Boy, J. Bogusz, Estimates of vertical velocity errors for IGS ITRF2014 stations by applying the improved singular

spectrum analysis method and environmental loading models, Pure Appl. Geophys. (2017) 1–18, https://doi.org/10.1007/s00024-017-1494-1.
[70] H. Steffen, C. Brandes, R. Steffen, P. Wu, Glacially Induced Seismicity in Europe, Geodesy Geodyn. 9 (3) (2018).
[71] C. Brandes, H. Steffen, R. Steffen, P. Wu, Intraplate seismicity in northern Central Europe is induced by the last glaciation, Geology 43 (2015) 611–614, https://doi.org/10.1130/G36710.1.
[72] C. Braitenberg, C. Shum, Geodynamic implications of temporal gravity changes over Tibetan Plateau, Ital. J. Geosci. 136 (2017) 39–49, https://doi.org/10.3301/IJG.2015.38.
[73] A. Gessert, T. Schicht, R. Koehler, Technical Possibilities and Developments For Seismological Long-Term Monitoring in Underground and Surface Mining, Geodesy Geodyn. 9 (3) (2018).
[74] C. Doglioni, E. Carminati, M. Crespi, M. Cuffaro, M. Penati, F. Riguzzi, Tectonically asymmetric Earth: from net rotation to polarized westward drift of the lithosphere, Geosci. Front. 6 (2015) 401–418, https://doi.org/10.1016/j.gsf.2014.02.001.
[75] F. Riguzzi, G. Panza, P. Varga, C. Doglioni, Can Earth's rotation and tidal despinning drive plate tectonics? Tectonophysics 484 (2010) 60–73, https://doi.org/10.1016/j.tecto.2009.06.012.
[76] C. Doglioni, E. Carminati, M. Cuffaro, D. Scrocca, Subduction kinematics and dynamic constraints, Earth Sci. Rev. 83 (2007) 125–175, https://doi.org/10.1016/j.earscirev.2007.04.001.
[77] P.J.M. Cerveira, J. Boehm, H. Schuh, T. Kluegel, A. Velikoseltsev, K.U. Schreiber, et al., Earth rotation observed by very long Baseline Interferometry and ring laser, Pure Appl. Geophys. 166 (2009) 1499–1517, https://doi.org/10.1007/s00024-004-0487-z.
[78] M. Tercjak, M. Rajner, A. Brzezinski, Monitoring High Frequency Earth Rotation by Ring Laser: on Modeling The Local Tilts, Geodesy Geodyn. 9 (3) (2018).
[79] J. Nastula, R. Weber, A. Brzezinski, A. Gruber, M. Kalarus, E. Umnig, A. Wielgosz, Ultra Rapid Oscillations in Earth Rotation Parameters Derived From GNSS Data, Geodesy Geodyn. 9 (3) (2018).
[80] J. Hagedoorn, O. Jenie, T. Nilsson, M. Karbon, H. Schuh, M. Madzak, et al., An Alternative Model for Short Period Ocean Tidal Variations of Earth Rotation (SPOT), Geodesy Geodyn. 9 (3) (2018).
[81] R.D. Ray, D.J. Steinberg, B.F. Chao, D.E. Cartwright, Diurnal and semidiurnal variations in the Earth's rotation rate induced by oceanic tides, Science 264 (1994) 830–832, https://doi.org/10.1126/science.264.5160.830.
[82] M. Schindelegger, D. Salstein, D. Einšpigel, C. Mayerhofer, Diurnal atmosphere-ocean signals in Earth's rotation rate and a possible modulation through ENSO, Geophys. Res. Lett. 44 (2017) 2755–2762, https://doi.org/10.1002/2017GL072633.
[83] R. Gross, Evaluating Tide Models for Operational Prediction of EOPs, Geodesy Geodyn. 9 (3) (2018).
[84] H. Schuh, Contributions of Geodesy to Monitoring Natural Hazards and Global Change, Geodesy Geodyn. 9 (3) (2018).
[85] J. Freymueller, Y. Fu, T. Jensen, Separating Surface Loading Deformation from Time-dependent Tectonic Deformation, Geodesy Geodyn. 9 (3) (2018).
[86] K. Heki, Y. Tu, D. Arisa, Geodetic Studies of Slow Slip Events in Subduction Zones with Active Back-Arc Opening, Geodesy Geodyn. 9 (3) (2018).
[87] M. Cheng, J. Ries, The unexpected signal in GRACE estimates of $$C_{20}$$ C 20, J. Geod. 91 (2017) 897–914, https://doi.org/10.1007/s00190-016-0995-5.
[88] M. Cheng, J.C. Ries, Decadal variation in Earth's oblateness (J2) from satellite laser ranging data, Geophys. J. Int. 212 (2018) 1218–1224, https://doi.org/10.1093/gji/ggx483.
[89] M. Cheng, Long Period Tide Variation from Satellite Laser Ranging (SLR), Geodesy Geodyn. 9 (3) (2018).
[90] M. Karbon, B. Soja, T. Nilsson, Z. Deng, R. Heinkelmann, H. Schuh, Earth orientation parameters from VLBI determined with a Kalman filter, Geod. Geodyn. 8 (2017) 396–407, https://doi.org/10.1016/j.geog.2017.05.006.
[91] J. Fernandez, J. Escayo, A.G. Camacho, J.F. Prieto, J.J. Mallorquí, Surface Deformation Study of La Palma Island Using C-Band Radar Imagery and GNSS Data, Geodesy Geodyn. 9 (3) (2018).
[92] L. Crescentini, A. Amoruso, What is Behind Campi Flegrei Inflations and Deflations? Clues From 35 Years of Geodetic Monitoring, Geodesy Geodyn. 9 (3) (2018).
[93] A. Amoruso, L. Crescentini, I. Sabbetta, Paired deformation sources of the Campi Flegrei caldera (Italy) required by recent (1980-2010) deformation history, J. Geophys. Res. Solid Earth 119 (2014) 858–879, https://doi.org/10.1002/2013JB010392.
[94] A. Amoruso, L. Crescentini, I. Sabbetta, P. De Martino, F. Obrizzo, U. Tammaro, Clues to the cause of the 2011–2013 Campi Flegrei caldera unrest, Italy, from continuous GPS data, Geophys. Res. Lett. 41 (2014) 3081–3088, https://doi.org/10.1002/2014GL059539.
[95] J. Mäkinen, I. Liepiņš, V. Sprogis, J. Sakne, K. Salmiņš, J. Kaminskis, et al., Using Relative Gravity Measurements Between Surface and Underground Stations to Assess the Hydrology of the Soil Layers in Between, Geodesy Geodyn. 9 (3) (2018).
[96] J. Hinderer, M. Calvo, S. Rosat, Y. Abdelfettah, G. Ferhat, U. Riccardi, et al., Hybrid Gravity Monitoring of a Geothermal Reservoir: a Case Study in Northern Alsace, France, Geodesy Geodyn. 9 (3) (2018).
[97] T. Abajo, J. Fernandez, J. Escayo, F. Luzon, P.J. Gonzalez, Surface Displacement Due to Groundwater Exploitation in the Lorca (Murcia, Spain) Region, Geodesy Geodyn. 9 (3) (2018).
[98] R. Bonì, G. Herrera, C. Meisina, D. Notti, M. Béjar-Pizarro, F. Zucca, et al., Twenty-year advanced DInSAR analysis of severe land subsidence: the Alto Guadalentín Basin (Spain) case study, Eng. Geol. 198 (2015) 40–52, https://doi.org/10.1016/j.enggeo.2015.08.014.
[99] C. Braitenberg, I. Nagy, B. Grillo, D. Zuliani, Plate Movement and Karstic Underground Water Flow in Fifty Years Of Ultra Broad Band Tilt Observations in the Karst- Implications For GNSS, Geodesy Geodyn. 9 (3) (2018).
[100] C. Braitenberg, T. Pivetta, G. Rossi, P. Ventura, A. Betic, Karst caves and hydrology between geodesy and archeology: field trip notes, Geod. Geodyn. 9 (2018) 262–269.
[101] D. Tenze, C. Braitenberg, I. Nagy, Karst deformations due to environmental factors: evidences from the horizontal pendulums of Grotta Gigante, Italy, Boll. Geofis. Teor. Appl. 53 (2012) 331–345, https://doi.org/10.4430/bgta0049.
[102] C. Braitenberg, G. Romeo, Q. Taccetti, I. Nagy, The very-broad-band long-base tiltmeters of Grotta Gigante (Trieste, Italy): secular term tilting and the great Sumatra-Andaman islands earthquake of December 26, 2004, J. Geodyn. 41 (2006) 164–174, https://doi.org/10.1016/j.jog.2005.08.015.
[103] G. Rossi, D. Zuliani, P. Fabris, Long-term GNSS measurements from the northern Adria microplate reveal fault-induced fluid mobilization, Tectonophysics 690 (2016) 142–159, https://doi.org/10.1016/j.tecto.2016.04.031.
[104] G. Rossi, P. Fabris, D. Zuliani, Overpressure and fluid diffusion causing non-hydrological transient GNSS displacements, Pure Appl. Geophys. (2017), https://doi.org/10.1007/s00024-017-1712-x.
[105] J.-P. Boy, Modeling River Storage From Radar Altimetry and Remote Sensing: validation Using GRACE and GPS, Geodesy Geodyn. 9 (3) (2018).
[106] H. Ruotsalainen, Recording Deformations of the Earth by Using an Interferometric Water Level Tilt Meter. Vol. Report S-53, Institute of Seismology, University of Helsinki, 2008.
[107] H. Ruotsalainen, Technical Details of the Modern Michelson-Gale Type Interferometric Fluid Level Tilt Meter of the Finnish Geospatial Research Institute, NLS, Finland, Geodesy Geodyn. 9 (3) (2018).
[108] H. Ruotsalainen, D. Bán, G. Papp, R. Leonhardt, E. Szücs, J. Benedek, Beyond Nanoradians? High Sensitivity Tilt Measurements in the Conrad Observatory, Austria, Abstr. IUGG Gen. Assem. 226–272015 Prague Czech Repub., 2015.
[109] V. Volkov, J. Mrlina, M. Dubrov, V. Polak, Observation of groundwater-related subsidence and thermal effects in tilt and strain measurements, G-ET2016 (2016).
[110] V. Volkov, J. Mrlina, M. Dubrov, V. Smirnov, S. Golovachev, V. Polak, Atmosphere and Ocean loadings and their interactions with the earthquake cycle, Geodesy Geodyn. 9 (3) (2018).
[111] G. Jentzsch, R. Schulz, A. Weise, Automated Burris gravity meter for single and continuous observation, Geod. Geodyn. 9 (2018) 204–209.
[112] H.R. Schulz, A new PC control software for ZLS-Burris gravity meters, Geod. Geodyn. 9 (2018) 210–219.
[113] S. Luo, J. Xu, Superconducting Gravimeter Calibration Using Earthquake Signal, Geodesy Geodyn. 9 (3) (2018).
[114] D. Crossley, M. Calvo, S. Rosat, J. Hinderer, More thoughts on AG-SG comparisons and SG scale factor determinations, Pure Appl. Geophys. (2018), https://doi.org/10.1007/s00024-018-1834-9.
[115] H. Wziontek, Verification of Transfer Functions of Co-Located Superconducting Gravimeters in Time and Frequency Domain, Geodesy Geodyn. 9 (3) (2018).
[116] A. Gebauer, PreAnalyseExtended: an Graphical Analysis Program for the Investigation of (Geophysical) Time Series, Geodesy Geodyn. 9 (3) (2018).
[117] S. Caldera, E. Realini, R. Barzaghi, M. Reguzzoni, F. Sansò, Experimental study on low-cost satellite-based geodetic monitoring over short Baselines, J. Surv. Eng. 142 (2016) 04015016, https://doi.org/10.1061/(ASCE)SU.1943-5428.0000168.
[118] D. Sampietro, S. Caldera, E. Realini, GeoGuard: an Innovative Service for Continuous Geodetic Monitoring by Means of Single-frequency GNSS Receivers, Geodesy Geodyn. 9 (3) (2018).
[119] P. Wessel, W.H.F. Smith, R. Scharroo, J.F. Luis, F. Wobbe, Generic Mapping Tools: Improved version released, EOS Trans. AGU 94 (2013) 409–410.

Prof. Dr. Carla Braitenberg, Ph.D. is Geophysics professor at the University of Trieste, Italy. She fulfilled her Physics and Geophysics education in Germany and Italy. She has found innovative ways to use geodetic measurements to describe geologic features. In a Karst environment gravity has proven useful to delineate the extent of caves, and is a tool to detect new ones. The underground karstic waterflows were shown to be detectable by their dynamic signal in geodetic measurements of deformation. Underground strainmeters and tiltmeters were shown to be very sensitive to the underground hydrology, and useful in describing the hydraulic characteristics of the subsurface waterflows. Exploiting the modern gravity satellite missions GRACE and GOCE she has worked on regional geologic structures and geodynamics, demonstrating how knowledge of the big scale is essential to the interpretation of terrestrial observations at local scale. She develops software methodologies that aim at an intelligent integration of high resolution terrestrial data with satellite observations optimizing investigative tools for natural resource exploration.